Numerical validation of a screw conveyor design method

Eugen Aschenbrenner* and Axel Funke

Institute of Catalysis Research and Technology, Karlsruhe Institute of Technology, Karlsruhe

E-mail: eugen.aschenbrenner@kit.edu

Abstract

Auger reactors represent an interesting alternative to other common reactor types. For example the pyrolysis of biomass or plastics. However the scale-up and design of auger reactors remains a challenging topic. Even though the fundamental design has been applied for several decades, things like granular mixing and transport are still not fully understood. A lot of the research on the transport of screw conveyors is focused on single-screw setups. This leads to the reliance on empirical data or in-house experience for the reactor design. For that reason, it is important to develop reasonable guidelines and design tools that are based on scientific principles, which can then be further validated by experiments and simulations. In this work, findings from a dimensional analysis are combined with auger reactor design criteria that were developed in the 1960s based on extensive experimental work and that were only available in German literature up until now, and the resulting assumptions are then tested with the help of DEM Simulations.

Introduction

Screw Conveyors or screw feeders are commonly used in a wide range of industries to transport different types of granular material either horizontally or over different inclinations, as well as to feed material into a reactor. For example biomass particles like wheat straw into gasification or pyrolysis units. They can also be used as the reactor themselves, where they show a high potential for the pyrolysis of biomass and waste.[1] Advantages include the ability to achieve heating rates similar to fluidized beds[2] and the ability to operate at different inclinations.[3] But although the general design is quite simple, the underlying physical processes like mixing are quite complex and empirical data or in-house experience is used to design or scale up a screw conveyor.[4,5] Different experimental and theoretical studies were conducted to investigate this mixing and transport phenomena. From early works in the 1960s which focused among other things on volumetric efficiency,[6,7] to later works that investigated the operating conditions of double screw conveyors[8,9] or the scale-up effects.[10] A powerful tool to design or scale-up processes or systems is the dimensional analysis. With the help of the resulting dimensional numbers, the processes can be described or categorized. Fluid flows or other transport phenomena are commonly described by them, therefore most well-known dimensionless numbers like the Reynolds, Nusselt, Mach or the Prandtl Number are derived from there. In recent years due to the increase in computing power, numerical simulations became an attractive tool to aid in the research of granular transport. With the help of the Discrete Element Method (DEM), every particle in the system can be tracked individually, and can therefore help with getting information on the particle level. This makes it also computationally demanding for systems with a high amount of particles. For example, systems with more than $1 * 10^8$ can require multiple weeks of calculations.[11] With the help of DEM the mixing in a double screw reactor,[12] the effect of different operating conditions like the rotational speed, inclination and volumetric fill level,[13,14] or non-spherical particles were investigated.[15] Minglani et al.[16] offer a more comprehensive overview of the granular flow research. This work aims to use the dimensional analysis and compare the experimental data

that were done in Germany in the 1960s with the results from DEM Simulations. Old graphs were digitized to make them easier to compare and different screw pitches, mono-sized and multi-sized particle systems as well as single and double screw conveyor set-ups were tested, and their effect on the volumetric efficiency was investigated. This should lead to a better understanding of the design of screw conveyors and feeders.

Methods

DEM Simulation

To investigate the hypothesis, the Discrete Element Method (DEM) is used. It was introduced by Cundall and Strack[17] as a way to describe the flow and behavior of granular material. It uses Newton and Euler's second law of motion.[18]

$$m_i \frac{d\vec{v}_i}{dt} = \sum_{k \in CL} \vec{f}_{ik}^{p-p} + \vec{f}_i^{p-f} + \vec{f}_i^{ext} \tag{1}$$

$$I_i \frac{d\vec{\omega}_i}{dt} = \sum_{k \in CL} \vec{M}_{ik}^{t} + \vec{M}_{ik}^{r} \tag{2}$$

$\vec{v}_i$ is the translational and $\vec{\omega}_i$ the rotational velocity of the particle i. The term $\vec{f}_{ik}^{p-p}$ in the right-hand side of Newton's second law is the sum of the particle-particle interactions between two particles i and k. These can be further split up into direct contact forces or non-contact forces like electrostatics. $\vec{f}_i^{p-f}$ are the interactions between the particle and the surrounding fluid, which can be set to zero if the fluid has a low influence on the particle. The last term stands for possible external forces that act on the particle, the most common one being the gravitational force or electromagnetic forces. $\vec{M}_{ik}^{t}$ is the tangential torque and $\vec{M}_{ik}^{r}$ the rolling friction. A Hertz-Mindlin Contact model, and an alternate elastic-plastic spring-dashpot rolling friction model (epsd2) was used to simulate the contact forces. The particle-particle contact forces are split up into normal and tangential elastic and viscious

damping forces.

$$\vec{f}_{ik,c}^{p-p} = (k_n \delta_n + \gamma_n \vec{v}_n) + (k_t \delta_t + \gamma_t \vec{v}_t) \tag{3}$$

The δ's are the normal and tangential overlaps and $\vec{v}$ are the relative velocity components. The Hertz-Mindlin Model calculates the coefficients k_n, k_t, γ_n and γ_t the following way.

$$k_n = \frac{4}{3} E_{eff} \sqrt{R_{eff} * \delta_n} \tag{4}$$

$$\gamma_n = 2\sqrt{\frac{5}{6}} \beta \sqrt{S_n m_{eff}} \tag{5}$$

$$k_t = 8 G_{eff} \sqrt{R_{eff} * \delta_n} \tag{6}$$

$$\gamma_t = 2\sqrt{\frac{5}{6}} \beta \sqrt{S_t m_{eff}} \tag{7}$$

Further equations are listed in table 1. There ν is the Poisson's Ratio and e the coefficient of restitution. The tangential overlap or force is truncated so that $f_t \leq \mu_s f_n$ is fulfilled, with the coefficient of static friction μ_s.

Table 1: Definitions for the contact between two particles

Young Modulus	$\frac{1}{E_{eff}} = \frac{(1-\nu_i^2)}{E_i} \frac{(1-\nu_k^2)}{E_k}$
Shear Modulus	$\frac{1}{G_{eff}} = \frac{2(2+\nu_i)(1-\nu_i)}{E_i} \frac{2(2+\nu_k)(1-\nu_k)}{E_k}$
Radius	$\frac{1}{R_{eff}} = \frac{1}{r_i} + \frac{1}{r_k}$
Mass	$\frac{1}{m_{eff}} = \frac{1}{m_i} + \frac{1}{m_k}$
-	$\beta = \frac{\ln e}{\sqrt{\ln^2(e) + \pi^2}}$
normal Stiffness	$S_n = 2 E_{eff} \sqrt{R_{eff} \delta_n}$
tangential Stiffness	$S_t = 8 G_{eff} \sqrt{R_{eff} \delta_n}$

The epsd2 model adds an additional torque contribution to the rolling friction torque:

$$\vec{M}_{ik}^r = \vec{M}_{el}^r + \vec{M}_{diss}^r \tag{8}$$

$$\Delta \vec{M}_{el}^r = -k_r \Delta \theta_r \tag{9}$$

θ_r is the incremental relative rotation. k_r is the rolling stiffness, and for the epsd2 model is defined with the tangential stiffness k_t as

$$k_r = k_t R_{eff}^2 \tag{10}$$

Theory and Dimensional Analysis

If only the physical phenomena during the pyrolysis are investigated, in this case, the transport and mixing processes, the relevant parameters are dependent on the geometry of the reactor. The different parameters are shown in Figure 1. Different strategies can be applied to reduce the complexity and focus on the rate-defining steps. With the postulate that an even distribution of heat carrier and biomass particles is sufficient to achieve the high heating rates required for fast pyrolysis and that such a mixture is achieved upon transportation inside the auger reactor, the problem is reduced to that of transportation efficiency.[4,7]

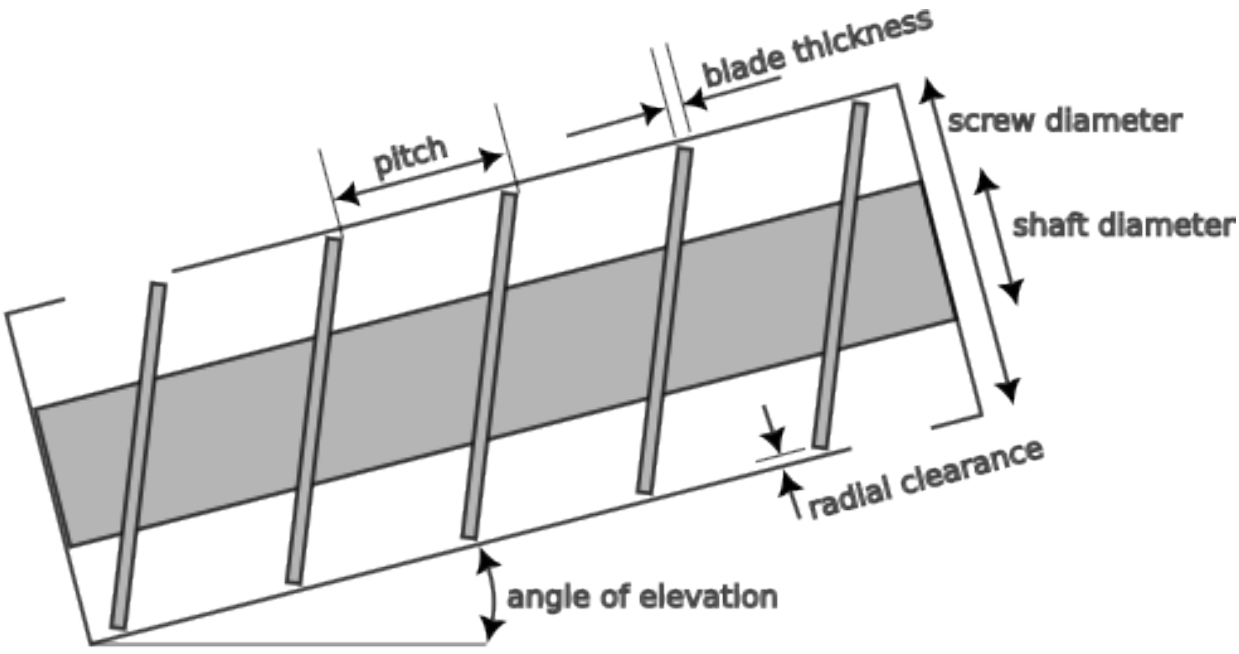

Figure 1: The different variables of the auger geometry

There were multiple studies done to investigate the transport of an auger reactor, most of these were done for a single screw reactor.[16] A common way to determine the efficiency

of the reactor is by measuring the actual volume or mass throughput and dividing it by the theoretical maximum throughput. If the volume is used it leads to the following equation

$$\eta_v = \frac{\dot{V}}{\dot{V}_{max}} \tag{11}$$

If all of the different variables of the auger geometry are taken into account and the screw is completely filled and the transported material is transported without slip, the maximum theoretical throughput can be calculated with the following formula:[6]

$$\dot{V}_{max} = \frac{\pi}{4}\left[(d+2c)^2 - d_w^2\right][h-t] \tag{12}$$

d and d_w are the diameters of the screw and shaft respectively. c is the radial clearance, h is the pitch of the screw and t is the width of the screw blades. To reduce torsional stress and a steep increase in power consumption, screw conveyors are in praxis filled up only between 15-45%, depending on how abrasive the feedstock is.[19,20] For the amount of throughput the rotating speed of the screw seems to have a bigger influence than the fill level itself[14] and the axial and average particle speed seem insensitive to the fill level.[13] To prevent jamming, it is recommended that the radial clearance is at least about 1.5 times larger than the biggest particle, and to reduce slipping back of the material, especially for elevated screws, it should not be bigger than 3 times.[21] The radial clearance has been reported to influence the performance of the screw reactor,[22] how much of it is just a result of changing the overall volume is not clear.

Previous Experiments

Interestingly, transport efficiency is a design criterion that was extensively investigated through experiments in the 1960s in Germany. In combination with the previously mentioned findings of the dimensional analysis and heat transfer/ mixing conditions inside an auger reactor, this turns out to be a promising tool to enable auger reactor design for fast

pyrolysis.[7] Because an auger reactor first of all needs to be able to transport the required material for the process, how the operating conditions and reactor dimensions influence the throughput needs to be investigated. There are a few basic assumptions that were stated in that work. One is that a double-screw reactor is equivalent to two single-screw reactors, that don't influence each other. The other is that the same granular material is used throughout all the experiments, and therefore the rolling coefficient can be ignored. Therefore, the throughput is only dependent on seven different variables. These are the gravity, radius of the screw, pitch, incline against the horizontal, speed of rotation and bulk weight as well as the actual throughput. Because the three SI units for length, mass and time occur, you can create four independent dimensionless numbers. The first one is the overall transport efficiency of the reactor, which is the ratio between the actual and the theoretical maximum throughput.

$$\eta = \frac{D}{D_{max}} \tag{13}$$

For the case of a slip-free transport and a completely filled reactor, the maximum throughput D_{max} can be described as:

$$D_{max} = n\gamma V \tag{14}$$

Subtracting the volume of the shaft but not the blades of the volume of either a single or double screw reactor, leads to the following equations for the Volume.

$$V_{double} = \frac{\pi}{2} h \left(d^2 - d_w^2\right) \tag{15}$$

$$V_{single} = \frac{\pi}{4} h \left(d^2 - d_w^2\right) \tag{16}$$

Inserting equation (14) and either (15) for the double screw or (16) for the single screw into (13) results in the following equations:

$$\eta_{double} = \frac{2D}{n\gamma\pi h \left(d^2 - d_w^2\right)} \tag{17}$$

$$\eta_{single} = \frac{4D}{n\gamma\pi h\left(d^2 - d_w^2\right)} \tag{18}$$

The second dimensionless number describes the steepness of the blades. For this, either the lead or the helix angle of the screw can be used. Here the Helix angle is used, which is calculated with

$$\tan\phi = \frac{\pi d}{h} \tag{19}$$

A higher value for the helix angle means steeper screw blades and a shorter pitch. Because of the effect of gravity, it is advisable to take the Froude number as the third dimensionless number. It was formulated as follows:

$$Fr = \frac{d\pi^2 n^2}{g} \tag{20}$$

The last dimensionless number is the incline of the whole reactor β itself. Combined they form a complete system, therefore the efficiency can be described as a function of the other dimensionless numbers $\eta = f\left(\beta; \tan\phi; Fr\right)$ Therefore, if the same pitch is kept and the reactors stay horizontal, the efficiency should only be dependent on the Froude number. To test his hypothesis, multiple experiments with different-sized screw mixers were conducted. For example 143 experiments with a smaller single screw and a diameter of 14.2 cm. Three different pitches and inclines were used and a large range of rotational speeds. The results are shown in Figure 2. A web-based program[23] was used to digitize the original graphs in order to make working with the original data easier.

The dots represent the individual experimental results, and they also show the curves that were fitted to the experimental results with the equation:

$$\eta = c_0 e^{-c_1 Fr} \tag{21}$$

As can be seen from the picture, shorter pitches or higher helix angles seem to favor transport efficiency. Those lie around 60-80% while the longer pitches are mostly around 5-20%

efficiency. For another experiment, which was not included in the graph, with a prototype that had a helix angle of $\tan\phi = 4.16$ it even stayed at around 90%. It can also be seen that for larger pitches the influence of the incline and rotational speed (or Froude number) is higher. The slope of the curve tends to get more horizontal, the shorter the pitch, or higher the helix angle is. Moreover, for the aforementioned prototype, it even seemed to be horizontal and therefore independent of the Froude number. With the help of the fitted curves, it can also be seen that the incline of the whole reactor has a bigger influence on the lower values. But in his work, it was mentioned that for $\tan\phi = 2.53$, there are irregularities for low Froude numbers around 0. The intersection of the fitted curve with the y-axis also seemed set a little too high, therefore the curves were refitted with Matlab,[24] the results are in Figure 3. This refitting led to a lower intersection point for the steepest screw of around 5-10 % and a lower negative slope. For the other two pitches, no significant differences were found. Nevertheless, the other graphs were not adjusted with this new value and the original slope and intersection data were used. Afterward, the values for the two constants c_0 and c_1 were plotted over the helix angle. Those are shown in Figure 4. For both constants, a higher angle leads to more similar values. For c_0 the experimental values for the other single (diameter = 8 cm) and the prototype double screw mixer (diameter = 21 cm) are shown. The curves for the different inclines converge for both constants. For $\tan\phi \to 0$ as well as $\tan\phi \to \infty$ the amount of material that is transported is almost zero, therefore a throughput maximum should exist. After inserting the equations and focusing only on the parts that are dependent on the pitch in the equation after it got solved for the throughput you get:

$$D' = \frac{\eta}{\tan\phi} \tag{22}$$

Using the results from the earlier experiments for the transport efficiency and inserting them in equation 22 leads to Figure 5. According to this graph, the highest throughput is at a pitch of around 2.3, and steeper pitches are less dependent on the Froude number. The graphs

show that lower Froude Numbers lead to higher throughput values, while the text mentions it the other way around. Most likely because the text refers to the actual throughput of the reactor, that increases, while the graph shows the calculated part of the throughput that is dependent on φ. With the help of equations 17 and 18, an existing screw can be scaled up. Keeping the same pitch, the shaft to screw diameter ratio, and the Froude Number at fixed number like $Fr = 1$, the earlier equations like 19 can be rearranged to $h = \frac{\pi}{\tan\phi} d$, $d_w = xd$ and $n = \sqrt{\frac{g}{\pi^2}} \frac{1}{\sqrt{d}}$. The scale-up graph for the prototype from Peters can be seen in Figure 6.

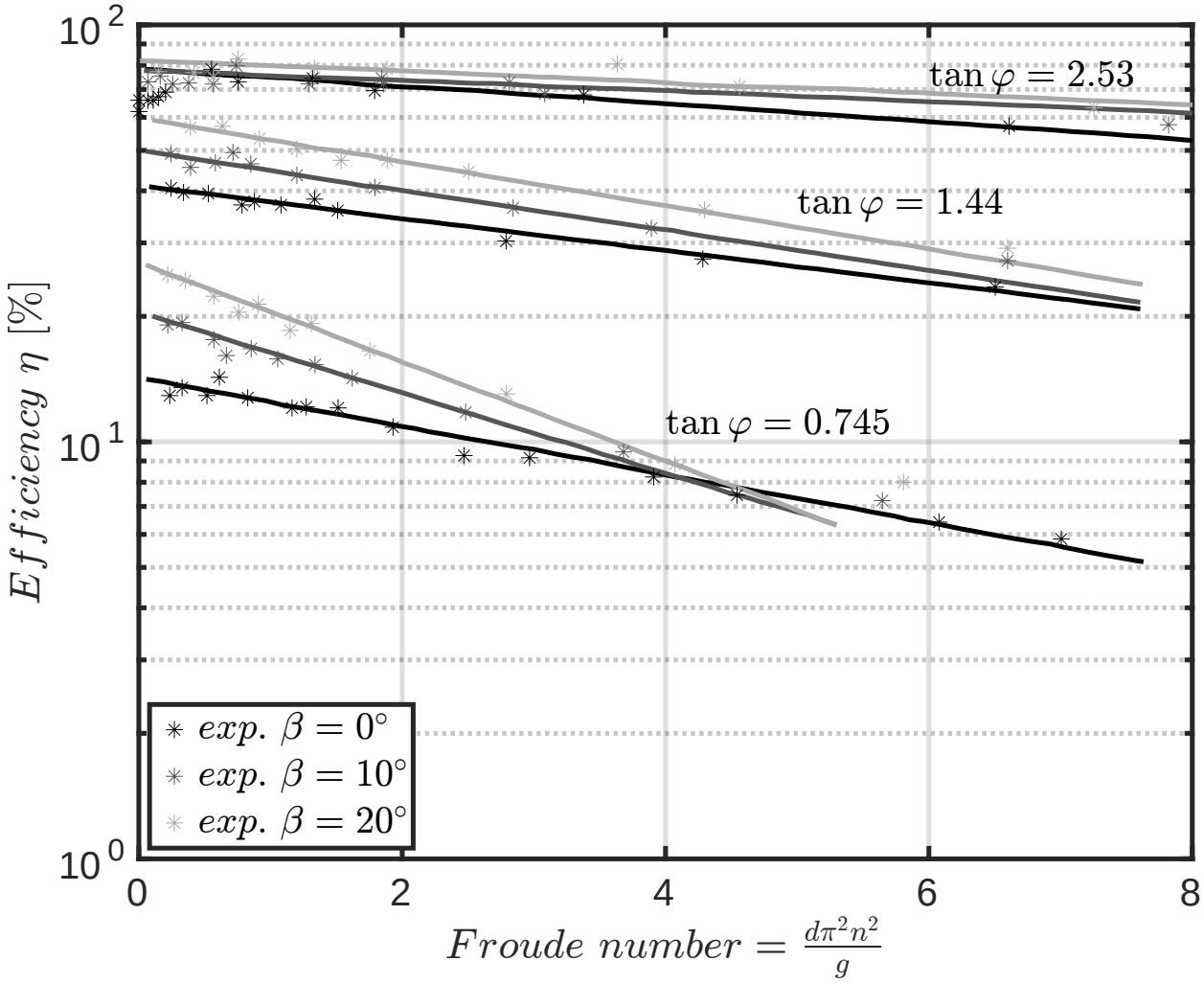

Figure 2: Digitized version of original experimental results of the efficiency (y-axis) over the Froude Number (x-axis) for different screw pitches. The y-axis is on a logarithmic scale. Three different pitches were used, as well as three different inclines. The points in the graph represent the individual experiments, and the lines are the fitted curves using equation (21)

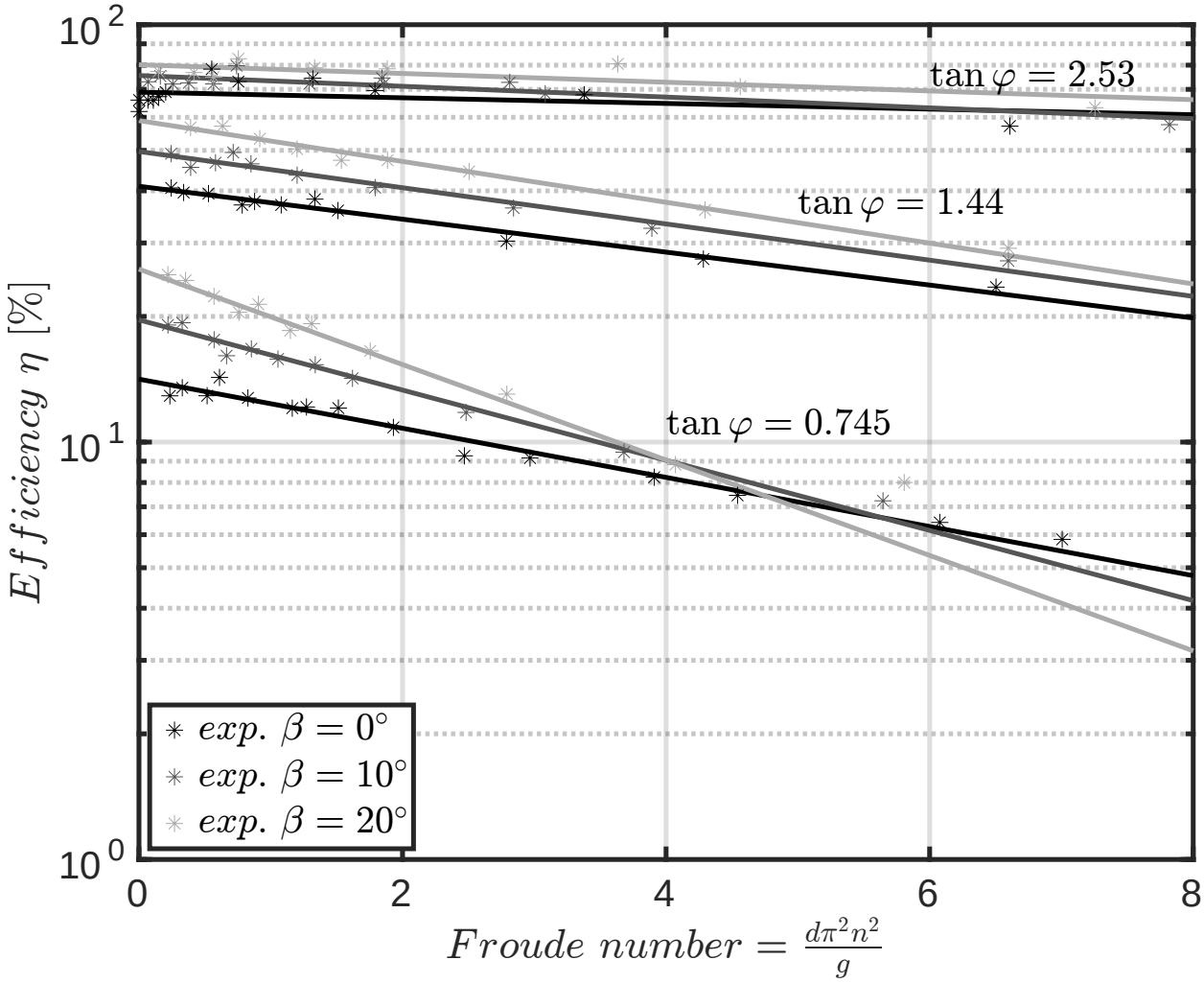

Figure 3: Digitized original experimental results similar to Figure 2, but the curves were refitted with Matlab, with the points from the original as a basis

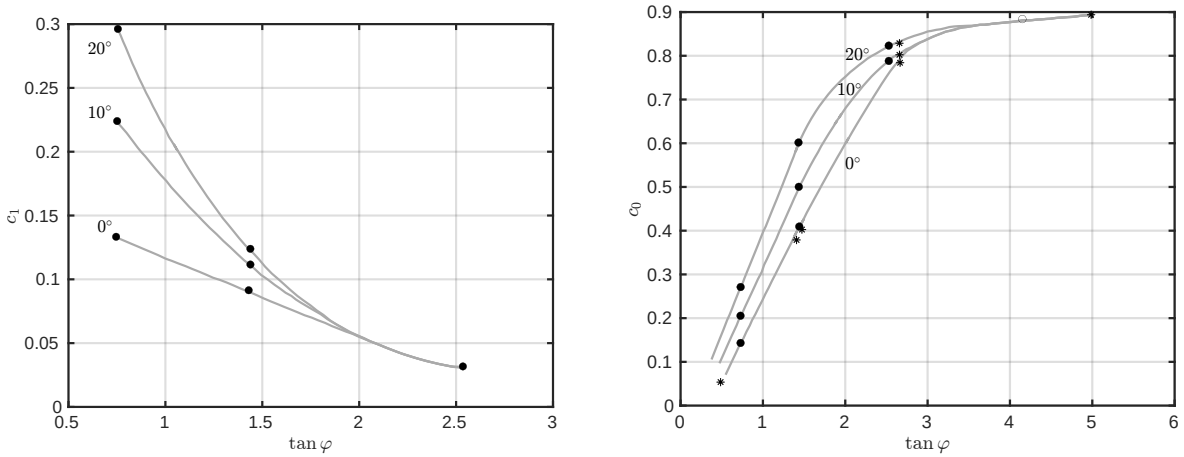

(a) c_1 (b) c_0

Figure 4: Digitized graph of the constants from the fitted curves with equation 21 in Figure 2 plotted over the helix angle. The 15 cm screw mentioned in the legend is the 14.2 cm one, the latter was the actual screw diameter and the 15 cm from the casing.[7]

Simulation Setup

The software that was used for the simulation is an academic LIGGGHTS version from the Johannes Kepler University (LIGGGHTS-PFM).[25] To count the particles and mass that go through a specified area, an existing function (fix massflow/mesh) from the software package was used. The different dimensions are shown in Table 2, with the first three being the ones that were used in the original experiments. The two smaller diameters were for the single screw setup, and the bigger prototype was a double screw. The helix angles that were used for the 8 cm screw were not directly mentioned and therefore the values were measured from the c_0 graph in figure 4. The basis for the simulation geometry is the PDU, with a diameter of 4 cm which has smaller dimensions compared to the 8, 14.2 and 21 cm screws used in the experiments. This should show if the transport behavior stays the same if the dimensionless numbers are still similar. The screw of the PDU at the KIT has two parts that differ in their pitch, a transport and a mixing area.

For the simulations for different screws with one continuous pitch, of which two corresponded to one of the original screw pitches of the PDU at the KIT.[2] These two can be seen in Figure 7. Corresponding to their part in the original screw, these will be called mixing

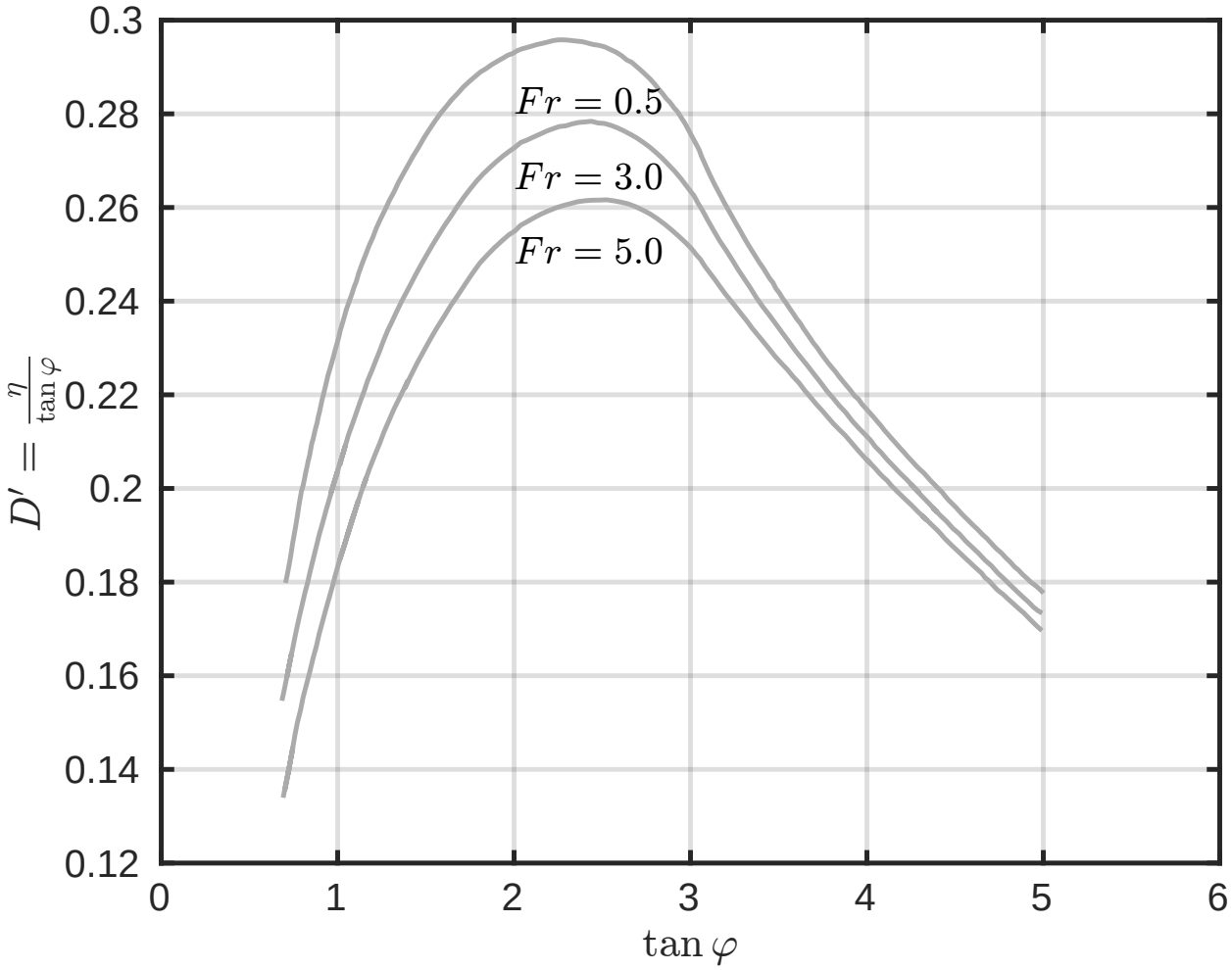

Figure 5: Digitized version of the partial throughput graph that is dependent on the pitch of the screw.[7]

Table 2: Screw Setup ups and diameters from the original experiments[7] and the simulation

diameter	8 cm
set-up	$\tan\phi$
single	≈0.5
single	≈1.4
single	≈1.5
single	≈2.6
single	5.0

diameter	14.2 cm
set-up	$\tan\phi$
single	0.745
single	1.44
single	2.53

diameter	21 cm
set-up	$\tan\phi$
double	4.15

diameter	4 cm
set-up	$\tan\phi$
s. & d.	0.63
s. & d.	1.44
s. & d.	2.73
s. & d.	5.0

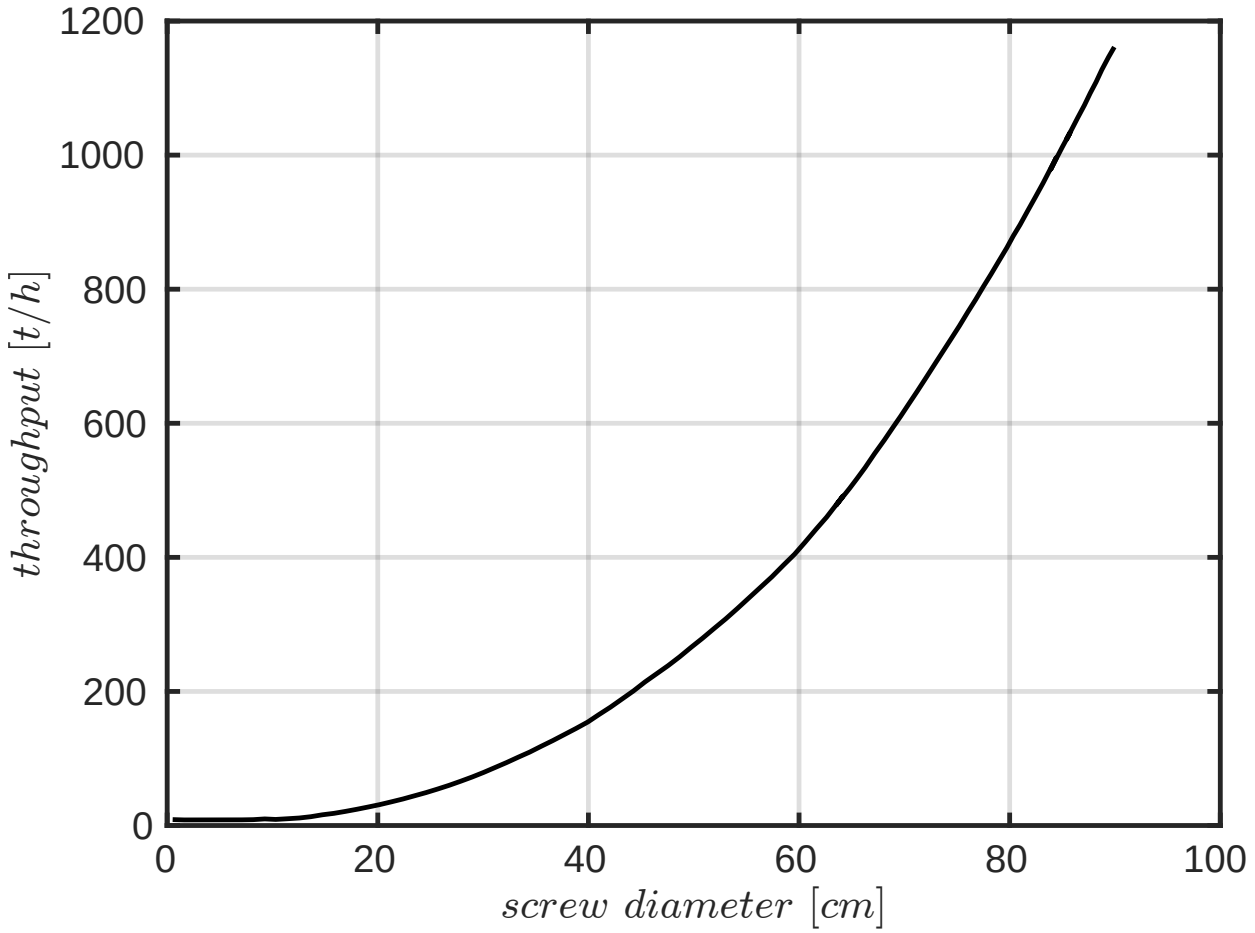

Figure 6: Digitized scale-up graph of the double screw reactor prototype.[7]

Table 3: Helix angle translated to pitch flight ratio $\frac{h}{d}$

$\tan\phi$	$\frac{h}{d}$
0.63	5
0.745	4.22
1.44	2.18
2.53	1.24
2.73	1.15
5	0.63

and transport screws in this work. In addition, two more screw variations that resemble the exact values as in the original work were used, which can be seen in Table 2. Table 3 shows the more commonly used pitch flight ratios to the corresponding helix angles. It can be seen that helix angles that are around ≈ 2.6 are close to the standard pitch. The frequencies that were simulated ranged from 0.75 to 12 Hz. The parameters for the bulk material derived from earlier works and are listed in Table 4.[26,27] Most of the experiments were done with steel spheres only, because the computation times when biomass was included were much longer than without. In general, it is expected that the particle size should not have a big influence on the axial speed of the individual particles,[5] but at least for powders, different levels of compressibility seem to have one on the mass flow.[28] Because of the low bulk density for the biomass, smaller absolute changes can change the calculated transport efficiency significantly. For the Young Modulus a lower value was chosen, which is a common practice to increase the time step and therefore reduce the computation time without influencing the bulk flow behavior.[29] The Young Modulus that was used equals $0.001E_0$, with E_0 being the actual value of the corresponding material, it was shown that there are no differences in the mixing behavior for values above $0.001E_0$.[30]

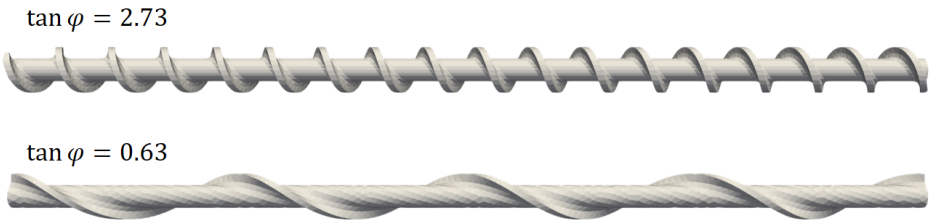

Figure 7: Two of the pitches that were used for the DEM Simulation. They are similar to the pitches that are seen in Figure 2. At the top is the "transport" and at the bottom is the "mixing" screw.

The simulation time step was $0.000002s$, which kept the Rayleigh time below 10 % and the Hertz time below 5 %. For the casing of the reactor stl-files were created, that acted as boundaries for the particles. The simulations were first run until they reached a quasi steady state, which acted as a initial condition. From that point onwards the mass

Table 4: DEM Parameters for the simulation

Parameter	Heat Carrier	Biomass
Youngs Module (MPa)	210	5
Poisson Ratio	0.3	0.035
Coefficient of restitution		
With Heat Carrier	0.9	0.6
With Biomass	0.6	0.2
With wall/screw	0.9	0.6
Coefficient of friction		
With Heat Carrier	0.2	0.3
With Biomass	0.2	0.9
With wall/screw	0.2	0.3
Coefficient of rolling friction		
With Heat Carrier	0.1	0.3
With Biomass	0.3	0.7
With wall/screw	0.1	0.3
Density (kgm^{-3})	7878.4	360
Bulk density (kgm^{-3})	4700	100
Radius (m)	0.001	0.003-0.007

flows were measured and averaged over a period of time. At higher frequencies the steady state was reached faster. Most of the previous experiments were done with a single-screw setup. Therefore a single and double screw mixing-reactor was simulated, to investigate differences in the transport efficiency. But instead of three different inclinations, only a horizontal setup was simulated. The double screw was run in a co-rotating setup, according to Kingston and Heindel,[8] there is a difference in mixing between co-rotating and counter-rotating up- or downward. Therefore, there is a possibility that there is a difference in the transport efficiency but this was not investigated in this work. The amount of particles in the simulation domain depended on the multiple factors like particle type, reactor volume and the screw pitch. Just filled with steel they ranged from 30000 to 100000 for the single screw and from 200000 to 275000 for the double screw. Filled just with biomass, the single screw had between $200000 - 500000$.

Results and discussion

Evaluation of single screw setup

In Figure 10 is the comparison between the simulated results and the experimental results. Although the pitches are not the same for every pitch, it was expected that the results should be still similar because of the relative similarity. As can be seen in the graphic, especially the results for the lower pitches follow the fitted curves quite closely. For the smaller helix angles, there seems to be generally a bigger spread of the results for lower Froude Numbers, but this could also be because there were just in general more simulations done in that area and with more types or bulk material. The result for the transport screw seems generally more stable and less variable. This could also already be seen in the experiments, where the influence of the inclination has a bigger influence at lower pitches. Moreover, the influence of the Froude number seems to be lower for higher pitches as well. The results for the higher helix angles are lower than expected and hover around 60 % for the transport screw and lower Froude Numbers. Even when taking the adjusted fitting curves from Figure 3 into account, they lie below the expected 70 % value. Because the volume of a pitch reduces with rising helix angles, the flight width of the screw has an increasing effect on the volume. This can be seen in Figure 8, where the steepest screw angle has the biggest drop in volume, while the screw with $\tan\phi = 0.63$ is barely influenced by it. Also for screws with smaller diameters, the volume decreases more with wider flights. This shows why Peters mostly didn't need to take it into account because he mainly worked with screws that are at least twice as large. The clearance has the opposite effect on the volume and increases it, but it is independent of the helix angle as can be seen in figure 9. Both the clearance and blade thickness have a higher influence on the overall volume for smaller screws with lower diameters. Doubling the diameter of the simulated screws, which becomes the same value for the smallest diameter Peter used in his work, decreases the Volume difference already by more than a half. The exact differences of course depend on the specific values for the

clearance and width. Depending on the exact setup, these two effects can cancel each other out.

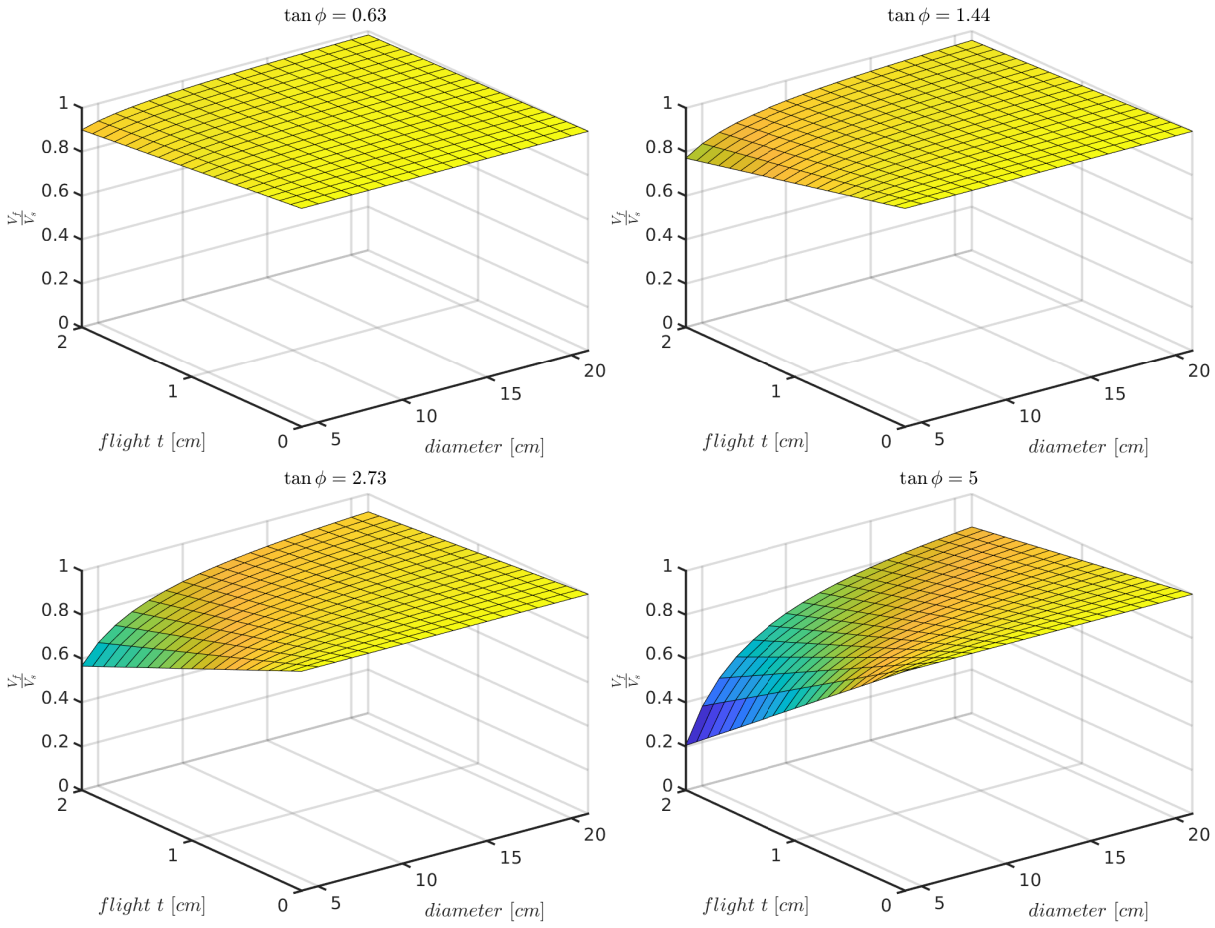

Figure 8: Change of the Volume if the width of the screw flight is taken into account. One axis is the total screw diameter, the diameter of the shaft is set to be always half of that. The clearance is set to 0, to see just the effect of changing the flight width.

Taking the flight width and radial clearance into account and calculating the theoretical maximum volume according to equation 12, leads to a theoretical maximum mass flow that is lower and the adjusted efficiency values are presented in figure 11. Now the values for the steeper pitch angles are in the area where the experimental results are. The trend of the values for the screw with $\tan\phi = 5$ stands out, because it has a rising trend in contrast to the other screws. But it generally seems that at some point, an increase in the helix angle does not increase the transport efficiency anymore or not much. From the dimensional analysis

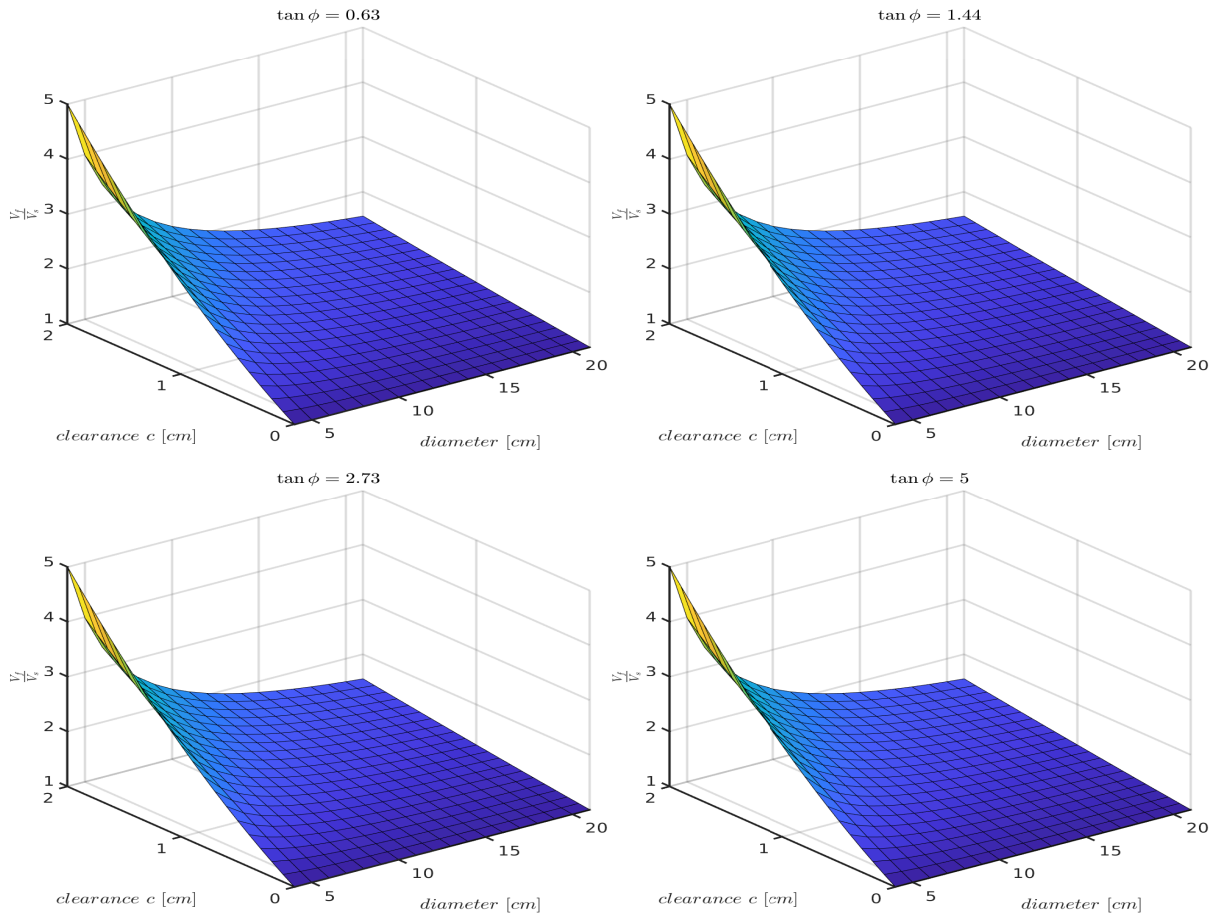

Figure 9: Change of the Volume if the clearance between screw and hull is taken into account. One axis is the total screw diameter, the diameter of the shaft is set to be always half of that. The flight width is set to 0, to see just the effect of changing the radial clearance.

expected transport efficiencies seem to hold true for different screw diameters.

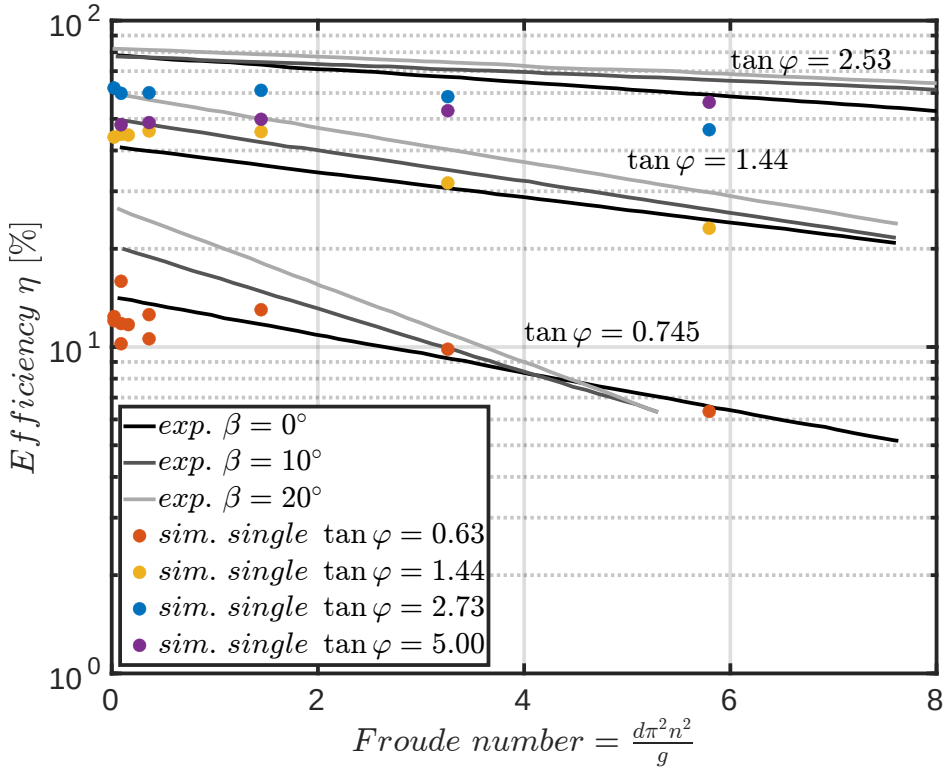

Figure 10: Comparison of results between DEM simulations and experimental results from Figure 2. The grey and black curves and points are the original experimental results with the unadjusted fitting curves. The colored points are the simulation results.

Evaluation of double screw setup

In Figure 12 is the comparison between the simulations of the double screw and the experimental results. In general, similar observations as for the single screw can be made. The mixing screw has a lower transport efficiency that the transport screw. The latter is similar to the single screw setup, also less influenced by the Froude Number and stays mostly the same. The efficiency of the mixing screw drops noticeably for higher Froude Numbers. Compared to the simulation results of the single screw setup, the transport efficiency of the double screw is higher for both pitches. This seems to suggest, that the assumption a double screw is just like two single screws in parallel that don't influence each other does not seem to hold true. The efficiency for the transport screw is around 20 % higher in the double screw

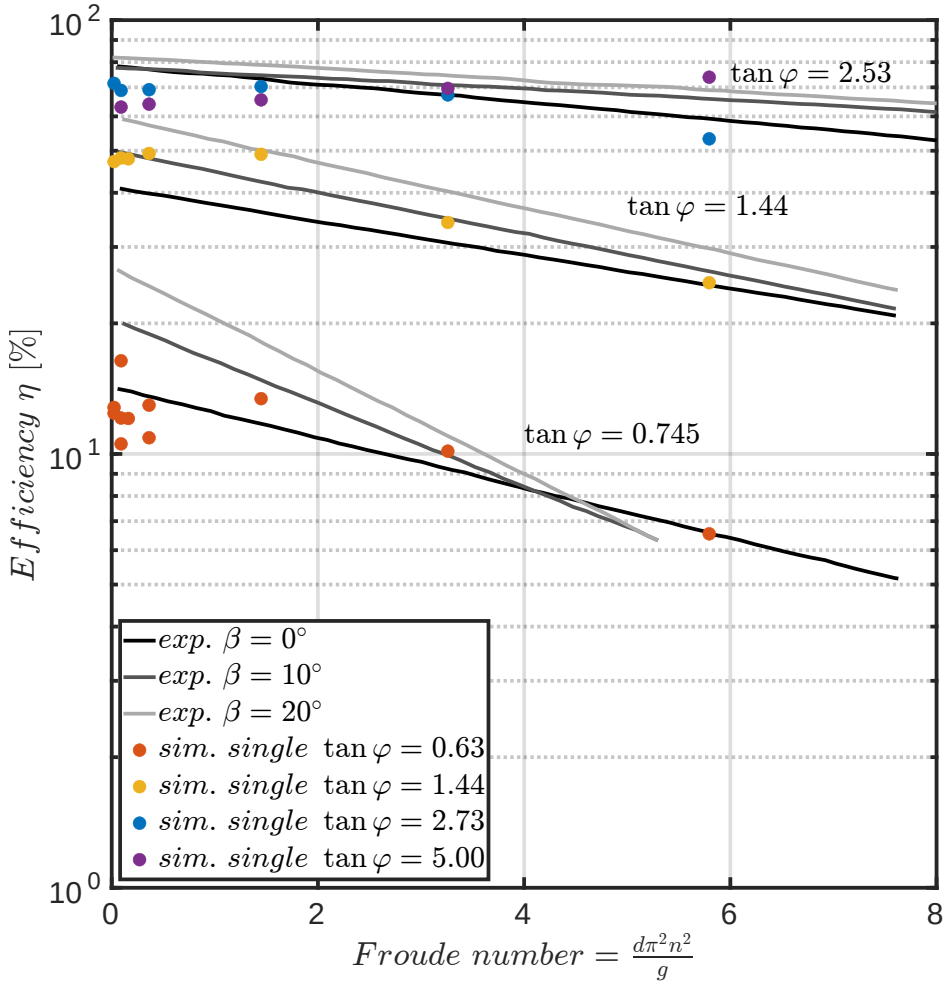

Figure 11: Comparison of results between DEM simulations and experimental results from Figure 2. The DEM results are adjusted with the volume calculation from Roberts and Willis.

setup, while for the mixing screw it is around 5-10 % higher. The results were also checked with the adjusted Volume, which takes the clearance and blade thickness into account and are plotted in Figure 13. Here the clearance has a big influence on the calculated volume, especially for the mixing screw. This brings the results closer to the expected values of the dimensional analysis, but the double screw seems still to be less influenced by the Froude Number. Especially the screw with $\tan\phi = 1.44$ has the biggest difference in curve slope compared to the single screw curve. The steeper screws are very close to each other and seem to trend to a maximum intersection point of around 70 %, which is lower than the 90 % from the experiments. Like mentioned earlier and seen in Figure 3, there were some irregularities for low Froude numbers and refitting the points with Matlab lowered the intersection point for steep curves in the experiments.

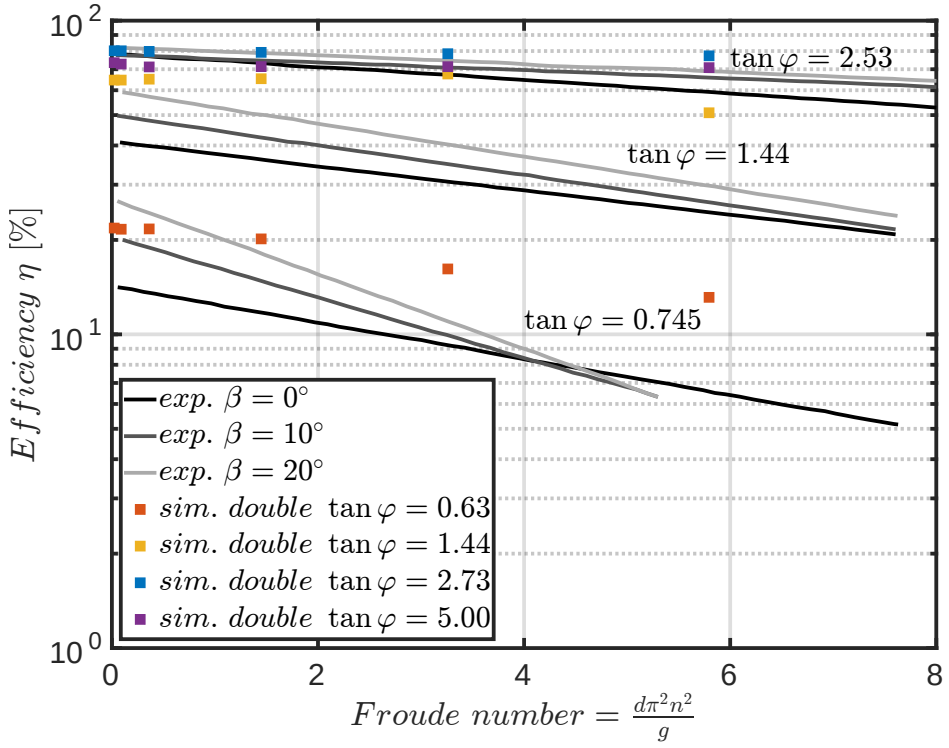

Figure 12: Comparison of the results between simulation of a double screw and experimental results from 2. The colored points are the simulation results for the double screw setup.

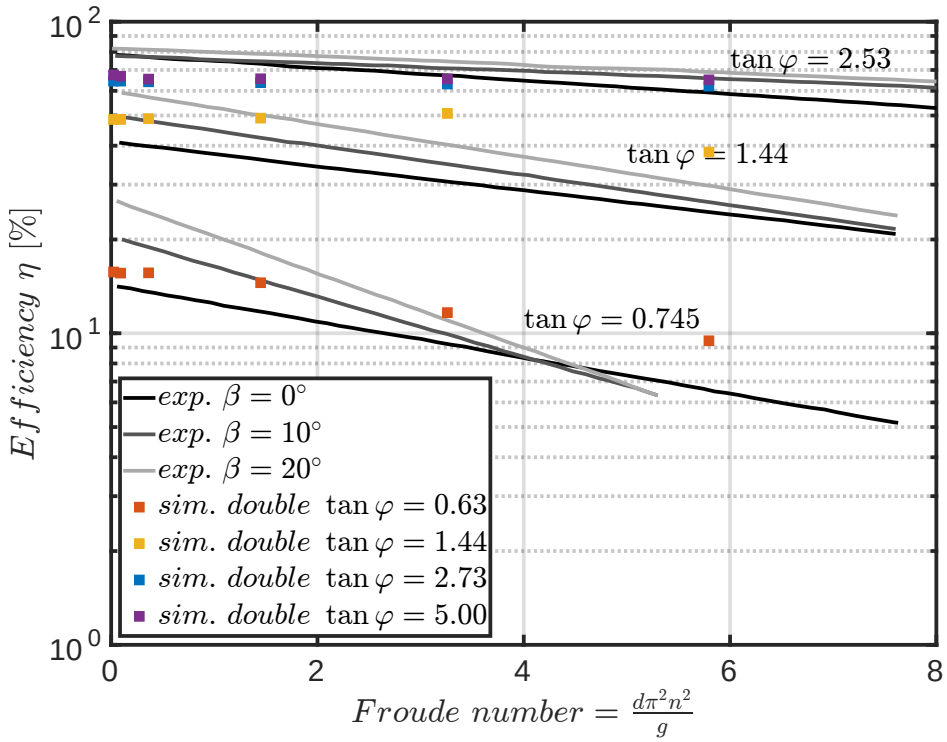

Figure 13: Comparison of the results between simulation of a double screw and experimental results from 2. The colored points are the simulation results for the double screw setup.

Evaluation of the constant c_0

To better illustrate the differences between the results, the constants that were shown in Figure 4 are used. In Figure 14 the comparison for the constant c_0 is shown, which is the intersection of the fitted curves with the y-axis. The simulation results with the adjusted Volume calculation, as well as the unadjusted ones, are plotted as colored dots. Because these are values from a fitted curve, the problem could also be, how exactly those are fitted to the experimental results. Especially the intersection with the y-axis could vary a lot, depending on where the curves are set. Even in the original, there is a cluster of results below the curve for low Froude Numbers, and Peters mentions in his work that for this pitch and low Froude Numbers close to 0, a lot of irregularities happened during the experiments. This could be seen with the new fit of the original values from Figure 3, which changes especially the curve for the steepest screw. Using those values would result in the the curve being lower between $\tan\varphi = 2 - 3$. The trend from the simulation results follows at the

start of the original curve, but for the steeper screws, it starts to decrease again and doesn't seem to trend toward 90 %. The adjusted curve for the single screw does not drop as much. The difference between the single and double screw decreases with the more detailed volume calculation.

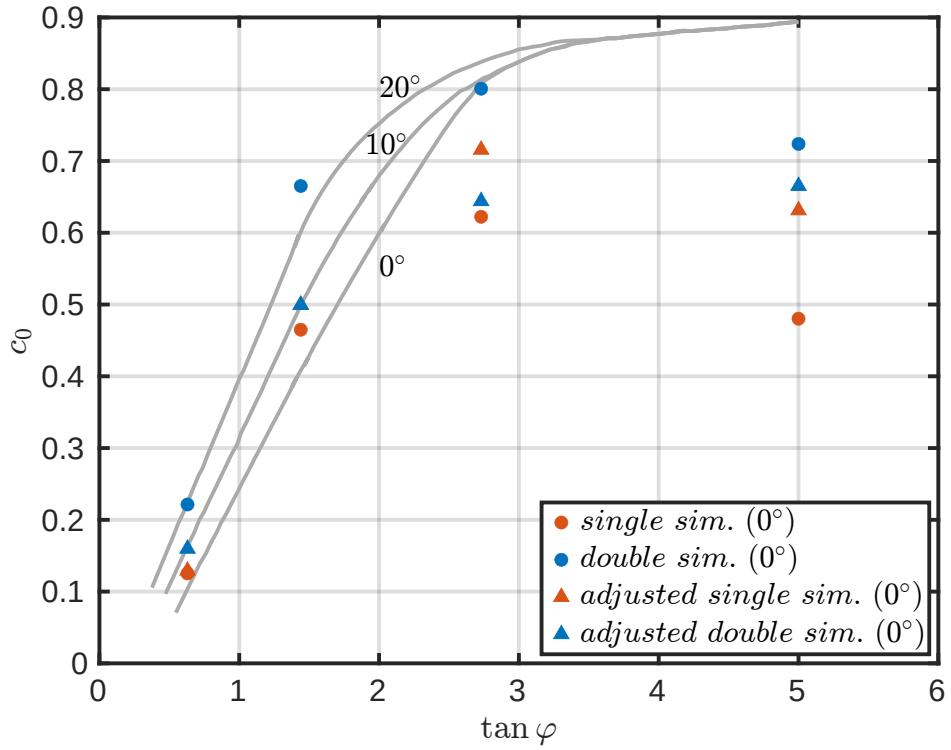

Figure 14: Comparison of the constant c_0 from the equation $\eta = c_0 e^{-c_1 Fr}$. The filled dots are from the main experiments of the single screw with a diameter of 14.2 cm. The stars are from single-screw experiments with a screw that has a diameter of 8 cm. The unfilled dot is from the original prototype, which is a double-screw setup with a screw diameter of 21 cm. The colored points are from the simulation results, one with the unadjusted volume (circles) and one with the adjusted volume (triangle)

Evaluation of constant c_1

Next will be the comparison of the constant c1 that represents the slope of the curves. In Figure 15 shows, that the single screw setup follows the predicted trend more closely than for the constant c0. Although the point for $\tan\phi = 1.44$ rises a bit, it generally seems to trend towards 0 for steeper screws. Even going below 0 for $\tan\phi = 5.0$, which is most likely

a simulation error. The same trend can be seen for the double screw, with the only difference that it the constant c_1 decreases quicker. In general for both setups the steeper screws are less influenced by the Froude Number, with almost no influence for very steep screws.

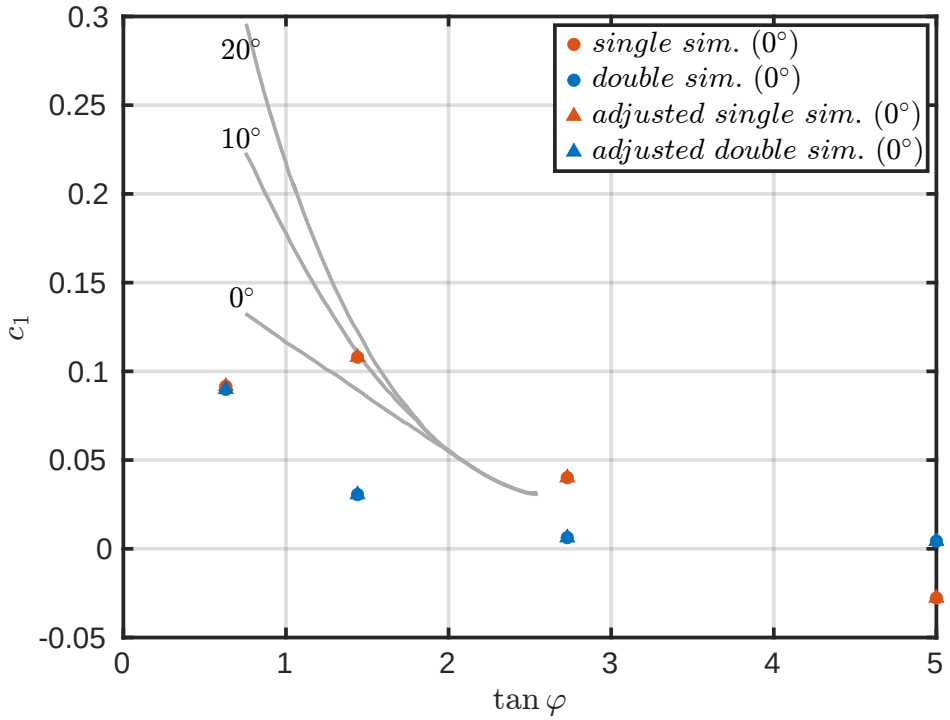

Figure 15: Comparison of the constant c_1 from the equation $\eta = c_0 e^{-c_1 Fr}$. In contrast to Figure 14, only the values from the 15 cm diameter single-screw setup are illustrated in the original.[7]

Design flow chart

With the developed equations from Peters, it is possible to either design an auger reactor from the ground up, or scale-up an existing one to the required throughput. An example flow chart is in Figure 16. If an existing screw is scaled-up, the different ratios should be kept constant. In the case of a new reactor, the pitch etc. that will be used should be defined. If the efficiency or the desired pitch was already investigated or is at least similar to one of them, the values for the efficiency from the graph can be used. Otherwise experiments or simulations with a smaller prototype can be conducted. However, the equations focus on the

mass flow. Other effects like mixing or heat transfer were not investigated and could change for bigger screws.

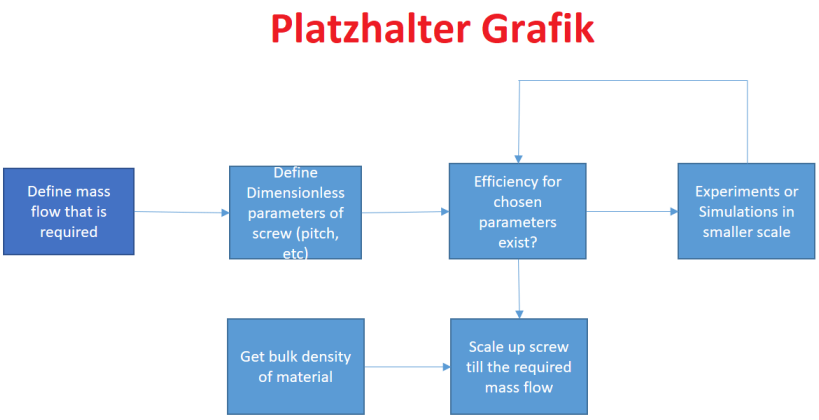

Figure 16: Design flow chart for scaling up or designing an auger reactor

Conclusion

In this study the transport efficiency of single and double screw auger reactors with different pitches were investigated, and compared with the results from Peters. Multiple DEM Simulations of the reactor were carried out with varying pitches and rotational speeds. Regarding the dimensional analysis, it could be seen that reducing the transport to only 7 variables was an oversimplification, at least for smaller screw diameters. The Volume differences that result from a flight width and radial clearance change have a significant effect on the calculated transport efficiency and need to be considered. But after taking those into account, the efficiencies are close to the expected results for most of the pitches, but the difference between the experimental values and the simulation results for very steep screws needs to be further investigated. Otherwise, the simulations follow the trends from the original experiments. That shows that with the help of the dimensional analysis, a few relevant variables could be determined, with which the expected throughput of a screw conveyor can be calculated. The developed dimensionless numbers offer therefore a powerful tool to design or scale an existing

screw reactor up or down. The comparison between single and double-screw setups, reveals that, although not completely correct, the assumption that a double-screw reactor can be seen as two parallel single screws holds somewhat true. The transport efficiency lies in a similar range to the corresponding single screw, but steeper angles seem to be less influenced by an increase in the rotational speed. This should allow to use the same design criteria for a single and double screw conveyor in regards to the mass throughput. If there are significant changes in the case when the rotation setup is changed from co- to counter-rotating, still needs to be investigated. Although a few simulations with non-uniformly sized particles were made, those were still spherical-shaped particles. How other particle shapes or material properties, especially from biomass, influence transport efficiency could be investigated in future studies.

Declaration of Competing Interest

The authors declare that they have no known competing financial interests or personal relationships that could have appeared to influence the work reported in this paper.

References

(1) Campuzano, F.; Brown, R. C.; Martínez, J. D. Auger reactors for pyrolysis of biomass and wastes. *102*, 372–409.

(2) Funke, A.; Grandl, R.; Ernst, M.; Dahmen, N. Modelling and improvement of heat transfer coefficient in auger type reactors for fast pyrolysis application. *130*, 67–75.

(3) Moser, K.; Wopienka, E.; Pfeifer, C.; Schwarz, M.; Sedlmayer, I.; Haslinger, W. Screw reactors and rotary kilns in biochar production – A comparative review. *174*, 106112.

(4) Funke, A.; Henrich, E.; Dahmen, N.; Sauer, J. Dimensional Analysis of Auger-Type Fast Pyrolysis Reactors. *5*, 119–129.

(5) Minglani, D.; Sharma, A.; Pandey, H.; Dayal, R.; Joshi, J. B. Analysis of flow behavior of size distributed spherical particles in screw feeder. *382*, 1–22.

(6) Roberts, A. W.; Willis, A. H. Performance of Grain Augers. *176*, 165–194.

(7) Peters, W. Schnellentgasung von Steinkohlen. Habilitationsschrift, Aachen, Techn. Hochsch., Aachen, 1963; Von der Fakultät für Allgemeine Wissenschaften der Rheinisch-Westfälischen Technischen Hochschule Aachen genehmigte Habilitationsschrift zur Erlangung der venia legendi; Habilitationsschrift, Aachen, Techn. Hochsch., 1963.

(8) Kingston, T. A.; Heindel, T. J. Granular mixing optimization and the influence of operating conditions in a double screw mixer. *266*, 144–155.

(9) Kingston, T. A.; Heindel, T. J. Optical visualization and composition analysis to quantify continuous granular mixing processes. *262*, 257–264.

(10) Marmur, B. L.; Heindel, T. J. Scale effects on double-screw granular mixing. *321*, 74–88.

(11) Blais, B.; Vidal, D.; Bertrand, F.; Patience, G. S.; Chaouki, J. Experimental Methods in Chemical Engineering: Discrete Element Method—DEM. *97*, 1964–1973.

(12) Qi, F.; Heindel, T. J.; Wright, M. M. Numerical study of particle mixing in a lab-scale screw mixer using the discrete element method. *308*, 334–345.

(13) Owen, P.; Cleary, P. Prediction of screw conveyor performance using the Discrete Element Method (DEM). *193*, 274–288.

(14) Wang, S.; Li, H.; Tian, R.; Wang, R.; Wang, X.; Sun, Q.; Fan, J. Numerical simulation of particle flow behavior in a screw conveyor using the discrete element method. *43*, 137–148.

(15) Sun, H.; Ma, H.; Zhao, Y. DEM investigation on conveying of non-spherical particles in a screw conveyor. *65*, 17–31.

(16) Minglani, D.; Sharma, A.; Pandey, H.; Dayal, R.; Joshi, J. B.; Subramaniam, S. A review of granular flow in screw feeders and conveyors. *366*, 369–381.

(17) Bandeira, A. A.; Zohdi, T. I. 3D numerical simulations of granular materials using DEM models considering rolling phenomena. *6*, 97–131.

(18) Norouzi, H. R.; Zarghami, R.; Sotudeh-Gharebagh, R.; Mostoufi, N. *Coupled CFD-DEM Modeling: Formulation, Implementation and Application to Multiphase Flows*; Wiley.

(19) Association, Conveyor Equipment Manufacturers *Screw Conveyors for Bulk Materials ANSI/CEMA Book No. 350-2015*; Conveyor Equipment Manufacturers Association (CEMA).

(20) KWS Manufacturing Company, L. Screw Conveyor Engineering Guide. `https://www.kwsmfg.com/wp-content/themes/va/pdf/Screw-Conveyor-Engineering-Guide.pdf`.

(21) Roberts, A. W. The influence of granular vortex motion on the volumetric performance of enclosed screw conveyors. *104*, 56–67.

(22) Burkhardt, G. J. Effect of Pitch, Radial Clearance, Hopper Exposure and Head on Performance of Screw Feeders. *10*, 0685–0690.

(23) Rohatgi, A. Webplotdigitizer: Version 4.6. `https://automeris.io/WebPlotDigitizer`.

(24) The MathWorks Inc. MATLAB Version: 9.8.0 (R2020a). `https://www.mathworks.com`.

(25) Department of Particulate Flow Modelling, J. LIGGGHTS-PFM Version: 23.02. `https://github.com/ParticulateFlow/LIGGGHTS-PFM`.

(26) Grandl, R. Simulation der Stoff- und Wärmetransportvorgänge bei der Schnellpyrolyse von Lignocellulose im Doppelschneckenmischreaktor.

(27) Kornmayer, C. Verfahrenstechnische Untersuchungen zur Schnellpyrolyse von Lignocellulose im Doppelschnecken-Mischreaktor. Ph.D. thesis, 35.02.02; LK 01.

(28) Falk, J.; Berry, R. J.; Broström, M.; Larsson, S. H. Mass flow and variability in screw feeding of biomass powders — Relations to particle and bulk properties. *276*, 80–88.

(29) Yan, Z.; Wilkinson, S. K.; Stitt, E. H.; Marigo, M. Discrete element modelling (DEM) input parameters: understanding their impact on model predictions using statistical analysis. *2*, 283–299.

(30) Chen, H.; Xiao, Y. G.; Liu, Y. L.; Shi, Y. S. Effect of Young's modulus on DEM results regarding transverse mixing of particles within a rotating drum. *318*, 507–517.